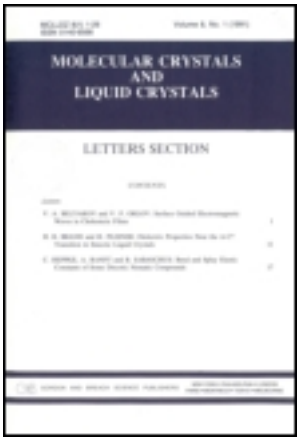

Molecular Crystals and Liquid Crystals
Publication details, including instructions for authors and subscription information:
http://www.tandfonline.com/loi/gmcl20

A New Exciton Blocking Material for Organic Solar Cell Applications

Gyeong Woo Kim [a], Raju Lampande [a] & Jang Hyuk Kwon [a]
[a] Department of Information Display, Kyung Hee University, Dongdaemoon-gu, Seoul, 130-701, Republic of Korea
Published online: 08 Jan 2014.

To cite this article: Gyeong Woo Kim, Raju Lampande & Jang Hyuk Kwon (2013) A New Exciton Blocking Material for Organic Solar Cell Applications, Molecular Crystals and Liquid Crystals, 585:1, 138-144, DOI: 10.1080/15421406.2013.851366

To link to this article: http://dx.doi.org/10.1080/15421406.2013.851366

Mol. Cryst. Liq. Cryst., Vol. 585: pp. 138–144, 2013

ISSN: 1542-1406 print/1563-5287 online
DOI: 10.1080/15421406.2013.851366

Taylor & Francis
Taylor & Francis Group

A New Exciton Blocking Material for Organic Solar Cell Applications

GYEONG WOO KIM, RAJU LAMPANDE,
AND JANG HYUK KWON*

Department of Information Display, Kyung Hee University, Dongdaemoon-gu, Seoul 130-701, Republic of Korea

We report a new efficient exciton blocking material, tris(2,4,6-trimethyl-3-(pyridin-3-l)phenyl) (3TPYMB), for organic solar cell applications. The introduction of 3TPYMB as an exciton blocking layer instead of well known BCP (2,9-dimethyl-4,7-diphenyl-1,10-phenanthroline) results in the significant improvement of short circuit current (Jsc) and open circuit voltage (Voc) in the boron subphthalocyanine (SubPC)/C_{60} based organic solar cell devices. As the results, the power conversion efficiency is enhanced by 11.8%. Such improvement with this new exciton blocking layer is mainly attributed to the good electron transportation by deep penetration of Al cathode metal to 3TPYMB layer.

Keywords Exciton blocking layer; exciton blocking material; organic solar cell; power conversion efficiency

Introduction

Recently organic solar cells (OSCs) have been received considerable attention due to their potential for light weight, low cost, and flexible applications [1,2]. However, current power conversion efficiency values of OSCs are still low for commercialization of real applications [3,4]. The crucial factors related performance improvements in OSCs are mainly efficient materials, active layer thickness, and morphologies of thin films. In addition to these factors, performances of OSCs can be also improved by using efficient functional layers such as exciton blocking layer (EBL) [5,6,7] and hole extraction layer [8,9]. The efficient EBL not only protect any damages of active layer from hot cathode metal atom during cathode deposition process but also confine the photo-generated excitons in the active layer, which results in enhanced performances in OSCs [10,11]. The exciton blocking layer can also work as an optical spacer [12]. Therefore, proper EBL thickness can increases light absorption amounts by redistribution of optical intensity within the active layer, which leads to increase of photocurrent of solar cell [13]. The proper functionalities of EBL material mainly depend on the charge transport property and sufficient band-gap. S. R. Forrest et al. reported that electrons in the large band-gap EBL move through the trap sites induced by the penetrated cathode metal atoms and the thickness of EBL is limited by the depth of penetration of

*Address correspondence to Prof. Jang Hyuk Kwon, Department of Information Display, Kyung Hee University, 1, Hoegi-dong, Dongdaemun-gu, Seoul 130-701, Korea. Tel.: (+82) 2-961-0948; Fax: (+82) 2-968-6924. E-mail: jhkwon@khu.ac.kr

metal [10,14]. The most widely used electron blocking material is BCP (2,9-dimethyl-4,7-diphenyl-1,10-phenanthroline). It has very deep HOMO level (−7.0 eV) and large band gap which helps to prevent quenching of exciton [15,16,17]. It has also an optically transparent characteristic in the visible region of solar spectrum and a good electron transport pathway through the penetrated metal cathode. Therefore, the improved performances in OSCs have been reported with BCP as exciton blocking layer [18].

In this paper, we report a highly efficient exciton blocking material for small molecule based OSC applications. This new exciton blocking material is optically transparent and enables OSCs to exhibit improved device performances compared with the most widely used BCP. We also report analysis of cathode metal penetration on different EBLs in OSCs by using the static time-of-flight secondary ion mass spectroscopy (TOF-SIMS) studies.

Experimental

In this study, we used 3TPYMB (tris(2,4,6-trimethyl-3-(pyridin-3-l)phenyl)borane), TmPyPB (1,3,5-tri[(3-pyridyl)-phenyl-3-yl]benzene), and BCP as exciton blocking materials. All materials were purchased from Luminescence Technology Corporation and ACROS Organics. Figure 1 shows the energy level diagram of fabricated OSCs and molecular structures of 3TPYMB, TmPyPB and BCP materials. The OSC devices were fabricated on commercially available indium-tin-oxide glass substrates having an active area of 2 mm×2 mm with a sheet resistance of 10 Ohm/square. The cleaned ITO glass was treated in ultraviolet ozone for 5 min. The OSC devices were fabricated on pre-cleaned ITO coated

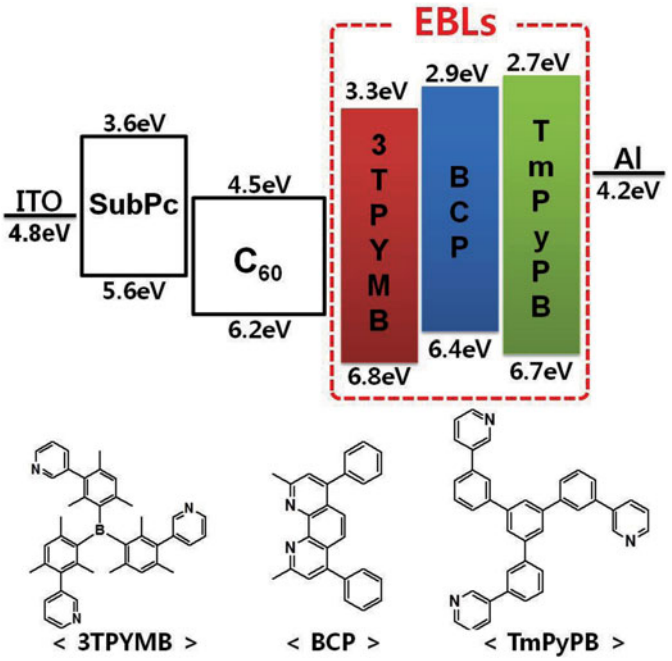

Figure 1. Energy level diagram of fabricated devices and molecular structures of EBLs.

glass substrates by the sequential thermal evaporation of boron subphthalocyanine (SubPc) and fullerene (C_{60}) as donor and acceptor and EBL followed by Al cathode (100 nm).

All organic materials were deposited under vacuum pressure of $\sim 3.0 \times 10^{-7}$ torr with a deposition rate of ~ 0.5 Å/s. Subsequently, Al (100 nm) was deposited in a vacuum chamber with a deposition rate of ~2.5 Å/s without breaking the vacuum and used as a cathode. The current density–voltage (J–V) characteristics of the fabricated devices were measured using a computer controlled Keithley 2400 source-meter in the dark and under illumination intensity of 100 mW/cm^2 with calibrated AM 1.5G sun simulator (Asahi Japan, Model HAL-302) in ambient conditions. A xenon light source was used to give simulated irradiance of 100 mW/cm^2 (equivalent to an AM1.5G irradiation) at the surface of the device. The J-V characteristic measurements were carried out in a dark chamber with a window slit of 5 mm^2 area for illumination. In order to investigate the penetration effect of cathode metal on EBLs static time-of-flight secondary ion mass spectroscopy (TOF-SIMS) study was carried out.

Results and Discussion

We fabricated three OSCs with different EBLs using thermal evaporation process. The fabricated OPV devices have following structures:

Device A: ITO/ SubPc (14.5 nm)/ C60(31.5 nm)/ BCP(8 nm)/Al(100 nm),
Device B: ITO/ SubPc((14.5 nm)/ C60(31.5 nm)/ TmPyPB (8 nm)/Al(100 nm), and
Device C: ITO/ SubPc((14.5 nm)/ C60(31.5 nm)/ 3TPYMB (8 nm)/Al(100 nm).

The device performances of SubPc(14.5 nm)/ C_{60}(31.5 nm) OSCs were investigated for three different EBLs with the same thickness (8 nm). For valid comparison we fabricated OSC device (Device A) with widely used BCP as an exciton blocking material and used as a reference device [8,9,19]. The wide band-gap electron transporting materials, TmPyPB and 3TPYMB were selected as new EBLs. The TmPyPB and 3TPYMB have sufficiently enough wide band-gap values as 4.0 eV [20] and 3.5 eV [21], respectively, whereas BCP has 3.4 eV band-gap value. Such wide band-gap characteristics of our all used EBL materials

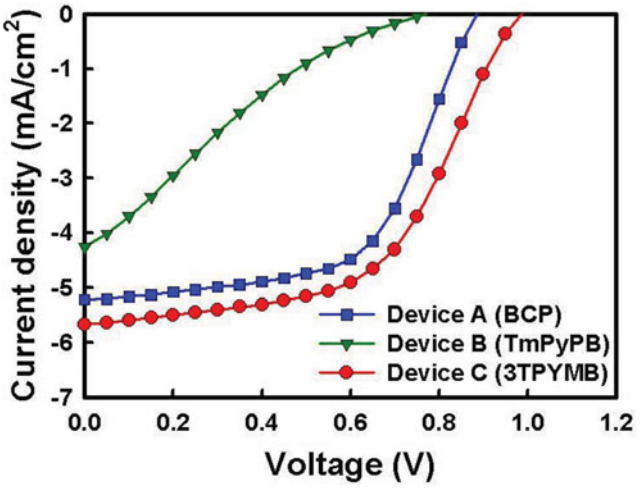

Figure 2. J-V characteristics of fabricated devices.

Table 1. Performances of fabricated OSCs with different EBLs

Device	V_{oc} [V]	J_{so} [mA/cm^2]	J_{sc} [mA/cm^2]	FF [%]	PCE [%]
A (BCP, 8 nm)	0.88	2.7×10^{-4}	5.22	58.5	2.70
B (TmPyPB, 8 nm)	0.77	8.54×10^{-3}	4.26	19.76	0.65
C (3TPYMB, 8 nm)	0.99	5.29×10^{-4}	5.67	54.1	3.02

are good to prevent light absorption loss from the EBL. The electron mobility values were reported as $\sim 10^{-3}$ cm^2/Vs and $\sim 10^{-5}$ cm^2/Vs for TmPyPB and 3TPYMB, respectively [17]. The Device A, B, and C are assigned for BCP, TmPyPB, and 3TPYMB exciton blocking materials, respectively.

Figure 2 shows J-V performances of fabricated OSCs with three different EBLs. The OSC with TmPyPB EBL (Device C) shows a power conversion efficiency (PCE) of 0.65%, while Device A and B with BCP and 3TPYMB shows overall better performances. The PCEs of Device A and C were 2.70% and 3.02%, respectively. The Table 1 shows the overall performances of fabricated OSCs with different exciton blocking layers. The short circuit current (Jsc) values were 5.22, 4.26, and 5.67 mA/cm^2 for Device A, B, and C, respectively. The open circuit voltages (Voc) were 0.88 V, 0.79 V, and 0.99 V, respectively. However, The Device C with 3TPYMB EBL shows the highest values of Jsc and Voc whereas Device B with TmPyPB EBL shows the lowest Jsc and Voc values. Although reported electron carrier mobility of TmPyPB is better than 3TPYMB, observed device performances of Device B are very poor and it also shows the s-shaped J-V curve. This illustrates that TmPyPB is unable to transport electrons from C_{60} to the cathode and charge carriers are accumulated at the interface between acceptor and TmPyPB layers [9]. It also indicates that 3TPYMB could transport electrons easily to cathode regardless intrinsic low carrier mobility and results in high Jsc and PCE in the device. We assume that the penetration of hot Al cathode may contribute to electron transportation in the 3TPYMB EBL. In order to understand more accurately for increased Voc in the Device C, dark saturation current (Jso) was investigated. Generally Voc is related to Jsc and Jso [7]. When Jso decreases, Voc is increased. When Jsc increases, Voc is also increased. The Fig. 3 shows the comparison of

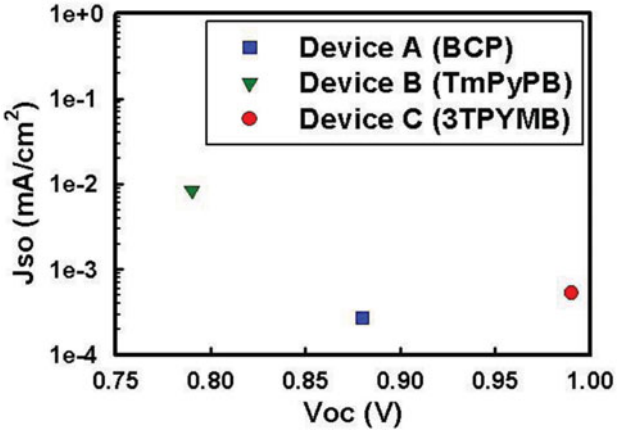

Figure 3. Reverse saturation current versus open circuit voltage characteristics of fabricated devices.

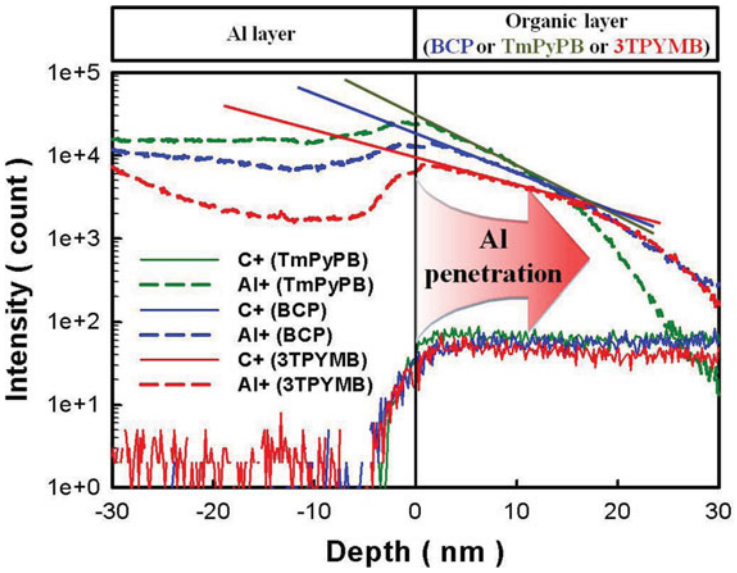

Figure 4. TOF-SIMS plots with different EBLs.

Jso characteristics with respect to Voc. The Jso values in Device A and C are very similar, however, Voc is changed significantly. This indicates that the Voc increase in Device C is mainly originated by Jsc improvement.

In order to observe the penetration effect of cathode metal in each EBL, TOF-SIMS analysis was performed. TOF-SIMS provides the detailed molecular information about surfaces, thin layer and its interfaces. Three samples were fabricated for the measurement of TOF-SIMS. The BCP, 3TPYMB, and TmPyPB were deposited on three different pre-cleaned ITO coated glass substrates followed by thermal deposition of 100 nm Al. Quantitative analysis with different samples is difficult because secondary ions yield strongly influenced by the chemical nature of surface and its chemical environment [22]. However we could compare the property of cathode metal penetration in each EBL by checking gradient profiles with respect to the depth of EBL. Figure 4 shows TOF-SIMS plots with different EBLs. The 3TPYMB shows the lowest depth profile of Al cation, while TmPyPB shows the highest depth profile. This means that Al penetration is strong in 3TPYMB layer, whereas TmPyPB have a strong blocking performance to Al penetration. These results are well consistent with device performances. The deep Al penetration to 3TPYMB layer improves device performances by efficiently extracting electrons from acceptor to cathode. On the contrary, Al penetration at the TmPyPB is too weak to efficiently extract electrons from acceptor. Since electron accumulation was generated at the interface between C_{60} and TmPyPB, therefore, it gives us poor device performances with a S-kinked curve [23,24].

To confirm the penetration effect of cathode metal, we fabricated Device B with different thickness of TmPyPB Layer. The optimized thickness of SubPc/ C60 was fixed as 14.5 nm and 31.5 nm respectively, whereas the thickness of TmPyPB was varied to 8 nm and 5 nm. The fabricated device structure was ITO/ SubPc (14.5 nm)/ C60 (31.5 nm)/ TmPyPB (8 nm & 5 nm)/ Al (100 nm). The Fig. 5 shows the J-V characteristics of fabricated devices under illumination intensity of 100 mW/cm^2 with calibrated AM 1.5G sun simulator in ambient conditions. The device with 5 nm EBL thickness shows increased efficiency and

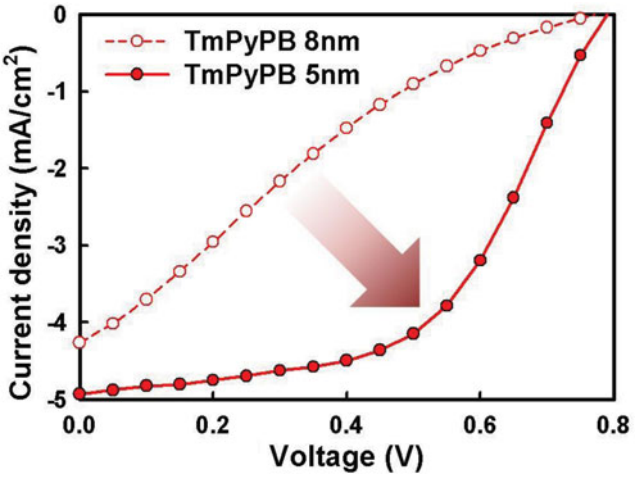

Figure 5. J-V characteristics of Bevice B with different thickness of TmPyPB.

FF as 2.08% and 53.42%, respectively, while device performances of the OSC with 8 nm EBL thickness show a low PCE of 0.65%. This result indicates that Al penetration depth is a crucial factor to determine electron transportation in the EBL.

The thickness optimization of 3TPYMB was carried out by varying their thickness values from 7 nm to 9 nm. The devices with 7 nm and 9 nm of 3TPYMB show about 30.3% and 16.3% decreases in the PCE, respectively. These results indicate that our originally used condition of 8 nm is the optimum thickness of 3TPYMB EBL.

Conclusions

In this study we have proposed that 3TPYMB is a highly efficient exciton blocking material. This 3TPYMB has a sufficient wide band-gap value of 3.4 eV to prevent the light absorption loss from the EBL. In addition, a low LUMO value (3.3 eV) with strong Al penetration to 3TPYMB EBL provides much improved electron transport characteristic, this results in increase of charge collection at the respective electrode. The power conversion efficiency of SubPc(14.5 nm)/ C_{60}(31.5 nm) OSC is improved by 11.8% with the introduction of 3TPYMB EBL as compare to the BCP. This EBL material will be very useful for achieving good performances in small molecule OSC devices.

Acknowledgments

This work was also supported by the Human Resources Development program (No. 20134010200490) of the Korea Institute of Energy Technology Evaluation and Planning (KETEP).

References

[1] Park, S. H., Roy, A., Beaupre, S., Cho, S., Coates, N., Moon, J. S., Moses, D., Leclerc, M., Lee, K., & Heeger, A. (2009). *Nat. Photonics*, *3*, 297.

[2] Chen, H.-Y., Hou, J., Zhang, S., Liang, Y., Yang, G., Yang, Y., Yu, L., Wu, Y., & Li, G. (2009). *Nat. Photonics*, *3*, 649.

[3] Gledhill, S. E., Scott, B., & Gregg, B. A. (2005). *J. Mater. Res.*, *20*, 3167.
[4] Nielsen, T. D., Cruickshank, C., Foged, S., Thorsen, J., & Krebs, F. C. (2010). *Sol. Energy Mater. Sol. Cells*, *94*, 1553.
[5] Gommans, H., Verreet, B., Rand, B. P., Muller, R., Poortmans, J., Heremans, P., & Genoe, J. (2008). *Adv. Funct. Mater.*, *18*, 3686.
[6] Rand, B. P., Li, J., Xue, J., Holmes, R. J., Thompson, M. E., & Forrest, S. R. (2005). *Adv. Mater.*, *17*, 2714.
[7] Liu, Y., Ren, Q., Su, Z., Chu, B., Li, W., Wu, S., Jin, F., Zhao, B., Yan, X., Wang, J., Fan, D., & Zhang, F. (2012). *Org. Electron.*, *13*, 2156.
[8] Kulshreshtha, C., Choi, J. W., Kim, J.-K., Jeon, W. S., Suh, M. C., Park, Y., & Kwon, J. H. (2011). *Appl. Phys. Lett.*, *99*, 023308.
[9] Kim, G. W., Jeon, W. S., Son, Y. H., Jung, S.-H., & Kwon, J. H. (2012). *Mol. Cryst. Liq. Cryst.*, *565*, 14.
[10] Hirose, Y., Kahn, A., Aristov, V., Soukiassian, P., Bulovic, V., & Forrest, S. R. (1996). *Phys. Rev. B*, *54*, 13748.
[11] Peumans, P., Bulovic, V., & Forrest, S. R. (2000). *Appl. Phys. Lett.*, *76*, 2650.
[12] Kim, J. Y., Kim, S. H., Lee, H. H., Lee, K. H., Ma, W. L., Gong, X. & Heeger, A. J. (2006). *Adv. Mater.*, *18*, 572.
[13] Lassiter, B. E., Wei, G., Wang, S., Zimmerman, J. D., Diev, V. V., Thompson, M. E., & Forrest, S. R. (2011). *Appl. Phys. Lett.*, *98*, 243307.
[14] Kim, I., Haverinen, H., Li, J., & Jabbour G. E. (2010). *Appl. Mater. Interfaces*, *2*, 1390.
[15] Yook, K. S., Jeon, S. O., Kim, O. Y., & Lee, J. Y. (2011). *Electrochem. Solid. St. Lett.*, *14*, 59.
[16] Chou, D. W., Huang, C. J., Wang, T. C., Chen, W. R., & Chen, K. L. (2009). *ECS Trans.*, *19*, 31.
[17] Xiao, L., Chen, Z., Qu, B., Luo, J., Kong, S., Gong, Q., & Kido, J. (2011). *Adv. Mater.*, *23*, 926.
[18] Huang, J., Yu, J., Lin, H., & Jiang, Y. (2009). *J. Appl. Phys. 105*, 073105.
[19] Son, Y. H., Kim, G. W., Jeon, W. S., Pode, R., & Kwon, J. H. (2012). *Mol. Cryst. Liq. Cryst.*, *565*, 8.
[20] Yang, X., Zhuang, S., Qiao, X., Mu, G., Wang, L., Chen, J. and Ma, D. (2012). *Opt. Express*, *20*, 24411.
[21] Goushi, K., Yoshida, K., Sato, K., & Adachi, C. (2012). *Nat. Photonics.*, *6*, 253.
[22] Benninghoven, A. (1994). *Angew. Chem. Int. Ed. Engl.*, *33*, 1023.
[23] Wanga, J. C., Ren, X. C., Shi, S. Q., Leung, C. W., & Chan, P. K. L. (2011). *Org. Electron.*, *12*, 880.
[24] Wagenpfahl, A., Rauh, D., Binder, M., Deibel, C., & Dyakonov, V. (2010). *Phys. Rev. B*, *82*, 115306.